Polyaniline–Rhodium Composites: Preparation, Physicochemical Characterization, and Catalytic Properties

Edyta Stochmal,[1] Magdalena Hasik,[1] Anna Adamczyk,[1] Andrzej Bernasik,[2] Wincenty Turek,[3] Agnieszka Sniechota[3]

[1]*Faculty of Materials Science and Ceramics, AGH—University of Science and Technology, 30-059 Kraków, Poland*
[2]*Faculty of Physics and Applied Computer Science, AGH—University of Science and Technology, 30-059 Kraków, Poland*
[3]*Department of Chemistry, Silesian Technical University, 44-100 Gliwice, Poland*

Received 10 May 2007; accepted 8 November 2007
DOI 10.1002/app.27679
Published online 28 December 2007 in Wiley InterScience (www.interscience.wiley.com).

ABSTRACT: In this work, polyaniline (PANI)–rhodium composites have been obtained for the first time. Their preparation procedure has involved reduction of Rh^{3+} ions in $RhCl_3$ aqueous solutions with $NaBH_4$ in the presence of PANI. Using UV–vis spectroscopy, it has been found that the reduction process is fast. X-ray diffraction and Rh3d XPS studies have confirmed that metallic rhodium is incorporated into PANI matrix. SEM and TEM investigations allowed to establish that the sizes of Rh crystallites formed depend on the amount of metal in the composite as well as on the preparation conditions. It has been demonstrated that the composites containing Rh nanoparticles whose size is predominantly below 10 nm can be obtained. IR spectroscopy has proved that PANI chain is protonated in the Rh^{3+} reduction process. Catalytic properties of PANI–Rh composites have been investigated using isopropyl alcohol conversion as the test reaction. It has been found that the composites containing Rh nanoparticles show high redox activity. Catalytic activity of the composites in which larger, agglomerated metal particles have been present is about three times lower. © 2007 Wiley Periodicals, Inc. J Appl Polym Sci 108: 447–455, 2008

Key words: polyaniline; rhodium; polymer-supported catalysts

INTRODUCTION

In modern technology, there is a constant need for new or improved materials. They should meet the growing and challenging requirements of, e.g., contemporary electronic devices. They are also necessary for chemical industry in which they can serve as raw materials or as catalysts. Development of new catalytic systems is particularly important since most industrial chemical processes are conducted in the presence of catalysts, mainly in heterogeneous conditions.[1]

In the search for new materials, composites play an important role. As multicomponent systems, they combine properties of their constituents. This makes it possible to overcome drawbacks of the substances when used alone. Therefore, in recent years significant scientific effort has been directed at the studies of various composite materials, particularly those containing polymers.[2–4]

Conjugated polymers, showing interesting optical, electrochemical, and electrical properties are attractive candidates for composite components. Among these polymers, polyaniline (PANI) is undoubtedly the most intensively investigated one nowadays. This is because of its simple synthesis by chemical or electrochemical methods and very good environmental stability.[5] PANI also exhibits interesting chemical properties. Unlike other conjugated polymers, it can be interconverted between undoped, that is nonconductive, and doped, that is conductive, states by acid treatment, often called protonation.[5] By choosing the appropriate acid, highly conductive, processible PANI can be obtained.[6,7]

In the literature, numerous studies devoted to the preparation of PANI containing composites are reported. Composites of PANI with conventional polymers, such as poly(methyl methacrylate),[7,8] cellulose acetate,[9] poly(vinyl chloride),[10] epoxy resins,[11] etc. have been prepared. They have been demonstrated to exhibit excellent optical properties[8] and very low percolation threshold for electrical conductivity (much below 1 wt % of PANI).[7,9–11] Compo-

Correspondence to: M. Hasik (mhasik@agh.edu.pl).
Contract grant sponsor: Polish Ministry of Scientific Research and Information Technology; contract grant number: 3T09A 003 26.

Journal of Applied Polymer Science, Vol. 108, 447–455 (2008)

sites of PANI with metal particles have also drawn considerable research interest in recent years. Ag,[12,13] Cu,[14] and Au,[15,16] have been incorporated into this polymer matrix. Sensing properties of PANI-Cu system towards chloroform vapors[14] and those of PANI–Au towards glucose[16] have been established.

There are also a number of articles devoted to PANI–platinum group metal composites. Such systems are very interesting because of the well-known catalytic properties of platinum group metals.[17] However, in the literature only the studies on PANI-Pt[18–23] and PANI-Pd[24–27] composites can be found. They have been prepared mainly by electrochemical means and their electrochemical and electrocatalytic properties investigated. There are significantly less artilcles describing chemical preparation of such composites.[20,21] Additionally, up to our knowledge, no studies have been devoted to incorporation of rhodium particles into PANI, even though rhodium is also an efficient catalyst.[28,29]

It should be noted that the amount of any material prepared electrochemically is always limited by the electrode surface. There is no such limitation in chemical syntheses. Hence, in the case of materials with potential technical applications, e.g. catalysts, chemical preparation is much more advantageous. Therefore, in the present work PAN-Rh composites have been prepared by chemical method. Physicochemical properties of the composites obtained have been characterized by X-ray diffraction, scanning and transmission electron microscopies (SEM and TEM, respectively), X-ray photoelectron spectroscopy (XPS), and Fourier transform infrared (FTIR) spectroscopy. It has been demonstrated that rhodium nanoparticles dispersed in PANI matrix can be obtained by a simple procedure when the appropriate preparation conditions are applied. Catalytic properties of PANI–Rh composites have been determined using isopropyl alcohol conversion as the test reaction. It has been shown that PANI–Rh composites containing mainly small (less than 10 nm in size) Rh particles exhibit high redox activity. Catalytic activity of the composites in which larger, less uniformly distributed metal particles are present is significantly poorer.

EXPERIMENTAL

Synthesis of PANI

In the studies, PANI in the emeraldine base form was applied as the matrix for incorporation of metallic Rh particles. The polymer was synthesized according to a modified method described in Ref. 30. Thus, freshly distilled aniline was oxidized with ammonium peroxydisulphate (molar ratio $n_{ox}/n_{an} = 0.25$) in 2*M* aqueous HCl solution. Polymerization was carried out for 4 h at 0°C. PANI hydrochloride thus obtained was washed with large amounts of HCl solution (1 : 10) and subsequently deprotonated in 0.3*M* aqueous ammonia solution for 48 h, then filtered, washed with water and methanol, and dried in dynamic vacuum.

Preparation of PANI–Rh composites

PANI–Rh composites were obtained in the one-step procedure. Rh^{3+} ions in $RhCl_3$ aqueous solution (0.67×10^{-3} or 3.8×10^{-3} mol/dm^3) were reduced with sodium borohydride in the presence of PANI. Molar ratio of the reducing agent to Rh^{3+} ions in all the reaction media was equal to 2.5. Samples of various Rh contents (0.05, 0.1, 0.2, 0.5, and 1 mol per 1 mol of PANI mer calculated as $C_{24}H_{18}N_4$) were prepared by changing the amount of $RhCl_3$ solution contacting with PANI. Thus, a typical preparation procedure of PANI–Rh composites adopted in the present work was as follows: 0.337 g (9.32×10^{-4} mol) of PANI was added to the appropriate amount of aqueous $RhCl_3$ solution to obtain the desired content of Rh in the composite. Subsequently, to the obtained suspension of PANI in $RhCl_3$ solution, sodium borohydride was added under vigorous magnetic stirring. Synthesis was carried out at room temperature for 2 h. Finally, the obtained product was filtered, washed with water, and dried.

During the syntheses of PANI–Rh composites, samples of the reaction mixture were collected, filtered and the UV–vis spectra of the filtrate solutions measured. This enabled us to monitor the process of Rh^{3+} ions reduction in the presence of PANI.

Characterization methods

X-ray diffraction studies were carried out on a Philips X'Pert XRD diffractometer using Cu Kα radiation.

Scanning electron microscopic analysis was performed on a Philips XL-30 microscope equipped with the EDS system.

TEM investigations were carried out using a Philips CM 20 microscope. The samples were placed on a carbon film deposited on copper grid.

UV–vis spectra in the range of 190–1100 nm were recorded on a Hewlett-Packard HP 8453 spectrophotometer equipped with a diode array detector.

XPS measurements were carried out using a VSW Manchester equipment and Al Kα radiation (1486, 6 eV, 200 W). Operating pressure in the analytical chamber was less than 5×10^{-8} mbar. Carbon C1s photoelectron peak originating from C—H or C—C groups was used for calibration and fixed at binding energy (B.E.) equal to 284.6 eV.

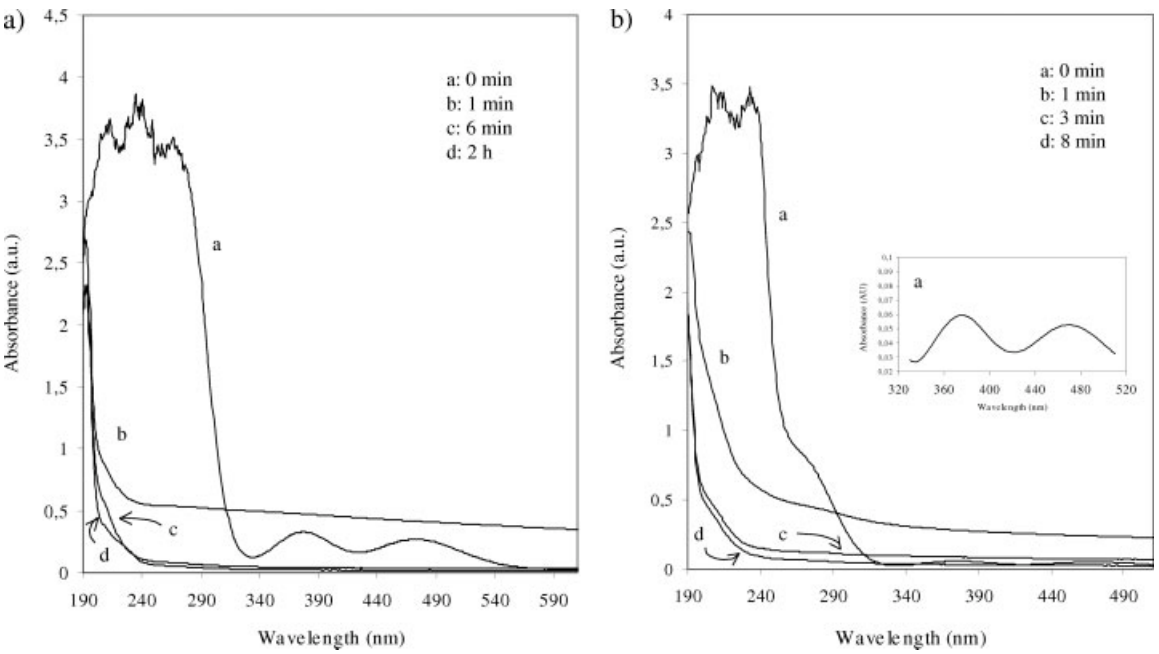

Figure 1 UV–vis spectra of the solutions contacting with PANI recorded during syntheses of PANI–Rh composites: (a) initial $RhCl_3$ concentration equal to 3.8×10^{-3} mol/dm^3; (b) initial $RhCl_3$ concentration equal to 0.67×10^{-3} mol/dm^3.

FTIR measurements in the middle infrared range (400–4000 cm^{-1}) in the transmission mode were performed on a BioRad FTS60v spectrometer using KBr pellet technique. The resolution of the experiments was equal to 4 cm^{-1}.

Investigations of catalytic properties

Catalytic properties of PANI–Rh composites were determined using isopropyl alcohol conversion as the test reaction. The experiments were conducted in the temperature range of 370–430 K, in the flow of nitrogen into which isopropyl alcohol was added; its molar ratio in the mixture was equal to 0.0179. In all the measurements, alcohol conversion degree was in the range of 5–15%. Catalytic reaction products were analyzed by gas chromatography. Based on the results, specific rates of the parallel reactions taking place in the systems, their activation energies as well as selectivities of isopropyl alcohol conversion towards acetone and propene were calculated.

RESULTS AND DISCUSSION

Reduction of Rh^{3+} ions in the presence of PANI

Rh^{3+} ions in aqueous solutions show distinct and characteristic absorption in the UV–vis spectral range. In these solutions, there exists a mixture of various Rh^{3+} aquachlorocomplexes. Based on the positions of absorption maxima it is possible to establish the major complex present in the solution.[31]

Analysis of the UV–vis spectra is a straightforward means to qualitatively follow Rh^{3+} ions reduction in the presence of PANI. This can be seen by examination of Figure 1 in which typical spectra of the $RhCl_3$ solutions contacting with the polymer recorded in the course of PANI–Rh composites syntheses are collected. The spectrum of the starting $RhCl_3$ solution of higher concentration (3.8×10^{-3} mol/dm^3) contains two absorption maxima in the visible range: at 377 nm and 472 nm. They correspond to the *d–d* electron transitions of Rh^{3+} ion in $[RhCl_3(H_2O)_3]$ complex.[31] Additionally, strong absorption in the UV range (190–300 nm) can be observed. It is connected with ligand-metal ion charge transfers in this complex.[31] Thus, the spectrum shows that $[RhCl_3(H_2O)_3]$ has predominated in the solution. In the case of the starting $RhCl_3$ solution of lower concentration (0.67×10^{-3} mol/dm^3), spectral features in the visible range are less distinct. However, closer inspection reveals the maxima at 375 and 470 nm [see the inset in Fig. 1(b)]. In the UV region, the shoulder at 275 nm and strong absorption between 190 and 250 nm are clearly visible. Thus, it can be concluded that in both $RhCl_3$ solutions used in the present work for the preparation of PANI–Rh composites, $[RhCl_3(H_2O)_3]$ complex has been the major one.

The UV–vis spectra change rapidly after addition of the reducing agent ($NaBH_4$) to the suspensions of PANI in $RhCl_3$ solutions. All the features originating from $[RhCl_3(H_2O)_3]$ vanish which proves disappearance of Rh^{3+} ions from the solutions due to their reduction. It is interesting to note that the spectra of

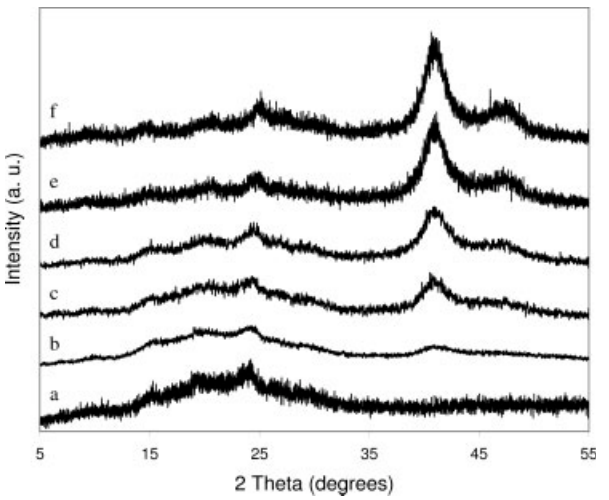

Figure 2 XRD patterns of (a): PANI and PANI–Rh composites containing different amounts of Rh and (b) 0.05; (c) 0.1; (d): 0.2; (e) 0.5; (f) 1.0 mol per 1 mol of PANI mer.

the samples collected in the initial periods of reduction (1 and 2 min) exhibit increased background. This indicates that small metal particles are present in the solutions. After 3 min of reduction, the background lowers and then it becomes completely flat which can be explained by the sorption of metallic rhodium on PANI. It should be also noted that—as indicated by the UV–vis studies—the rate of the Rh^{3+} ions reduction process is not influenced by the initial $RhCl_3$ concentration in the solution.

Hence, UV–vis spectroscopy shows that [$RhCl_3(H_2O)_3$] reduction with $NaBH_4$ taking place in aqueous solutions in the presence of PANI is fast. It occurs in the solution first. However, after a very short initial period, metal particles become trapped in the polymer matrix.

Physicochemical properties of PANI–Rh composites

Physicochemical investigations of PANI–Rh systems obtained have been performed to confirm the reduction of Rh^{3+} ions in the $RhCl_3$ solutions and to establish unequivocally incorporation of metallic rhodium into the polymer matrix. Additionally, these studies have been aimed at determining the sizes and size distributions of metal particles formed in the systems and at revealing their dependence on the preparation conditions, that is, on the starting concentration of $RhCl_3$ solution used in the experiments. Finally, we have been interested how PANI chain changes upon the Rh^{3+} ions reduction process since this could make it possible to establish if there are any specific interactions between the polymer and metallic rhodium particles. Interactions of PANI and metallic palladium have been postulated in the literature.[26]

Reduction of Rh^{3+} ions from the solutions resulting in the formation of metallic rhodium particles which are incorporated into PANI matrix has been confirmed by XRD studies. XRD patterns of PANI–Rh systems obtained together with that of the starting PANI are shown in Figure 2. As can be seen, all of the patterns contain both, broad reflections in the 2θ range between 12° and 35° and distinct, ''crystalline'' maxima at 2θ equal to 41° and 49°. The broad reflections in the 2θ range between 12° and 35° can be also observed in the XRD pattern of the starting PANI. Hence, they correspond to the amorphous polymer phase present in PANI–Rh systems. The ''crystalline'' reflections can be unequivocally ascribed to metallic rhodium crystallites.[32] It should be noted that the intensities of these reflections are related to the amount of rhodium present in the systems: the intensities grow as the content of rhodium in the samples increases. Thus, based on XRD studies it can be concluded that reduction of [$RhCl_3(H_2O)_3$] with $NaBH_4$ carried out in the presence of PANI leads to the formation of the two-phase systems in which metallic rhodium particles are dispersed within PANI matrix. Based on XRD patterns, the average sizes of rhodium crystallites present in the samples have been calculated using Scherer's equation. According to the results, the average size has only slightly differed for all the samples prepared and has been in the range of 3–6 nm. Thus, XRD diffraction studies suggest that in all the cases metal nanoparticles have been formed.

Although XRD unequivocally shows the presence of metallic rhodium in the systems, Rh3d XPS spectroscopy has been applied to verify if it is the only oxidation state of rhodium incorporated into PANI. A typical Rh3d XPS spectrum of PANI–Rh system is presented in Figure 3. It contains only one $Rh3d_{5/2-3/2}$ doublet of $Rh3d_{5/2}$ binding energy equal to 307.6 eV. This B.E. value corresponds to zerovalent rhodium.[33]

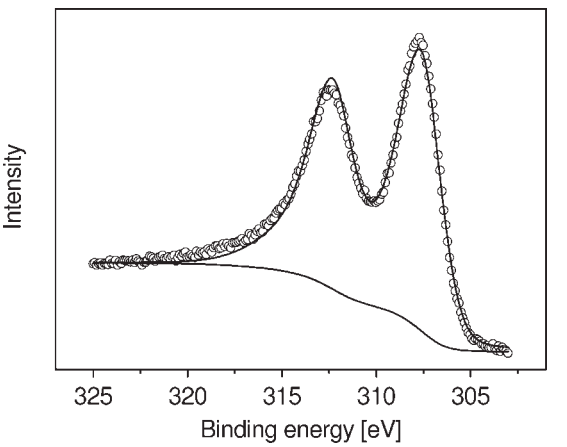

Figure 3 Rh3d XPS spectrum of PANI–Rh composite containing 0.1 mol Rh per 1 mol of PANI mer.

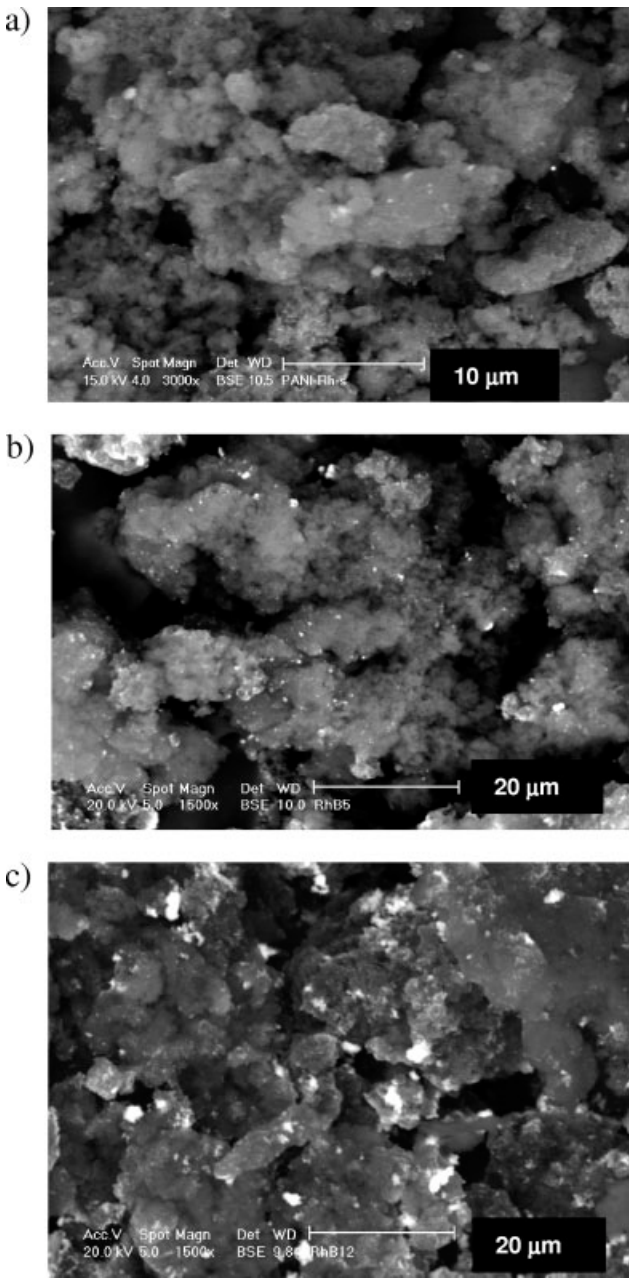

Figure 4 BSE images of PANI–Rh composites containing (a) 0.05, (b) 0.2, (c) 0.5 mol Rh per 1 mol of PANI mer prepared in the solution of initial $RhCl_3$ concentration equal to 3.8×10^{-3} mol/dm^3.

Hence, XPS results prove that all rhodium has been incorporated into PANI in the zerovalent, that is, metallic state.

The sizes of rhodium particles present in PANI–Rh composites prepared have been also determined by scanning and transmission electron microscopic studies. BSE images of representative PANI–Rh samples containing various amounts of rhodium are presented in Figure 4. White spots of irregular shapes are visible in the micrographs. The number and size of the spots occurring in the samples depend on the total amount of rhodium. They are numerous and significantly larger in the composites of higher Rh contents. In the BSE images of the samples containing the lowest Rh amount (0.05 mol Rh per 1 mol of PANI mer), white spots are few and significantly smaller. As has been established by X-ray microanalysis, in the spots rhodium is present. X-ray microanalysis, however, is not able to distinguish between various oxidation states of the elements. Nevertheless, in view of X-ray diffraction and Rh3d XPS results, it is clear that the white spots in BSE images of PANI–Rh composites correspond to metallic rhodium particles. Their size is in the range of 0.5–1.5 and 0.5–3.5 μm in the samples containing 0.2 and 0.5 mol Rh per 1 mol of PANI mer, respectively. Irregular shapes suggest that they are aggregated smaller rhodium particles.

In the case of the samples containing the lowest Rh amount (0.05 mol Rh per 1 mol of PANI mer), the use of transmission electron microscope has proved particularly useful. Figure 5 shows TEM images of the samples prepared in the $RhCl_3$ solutions

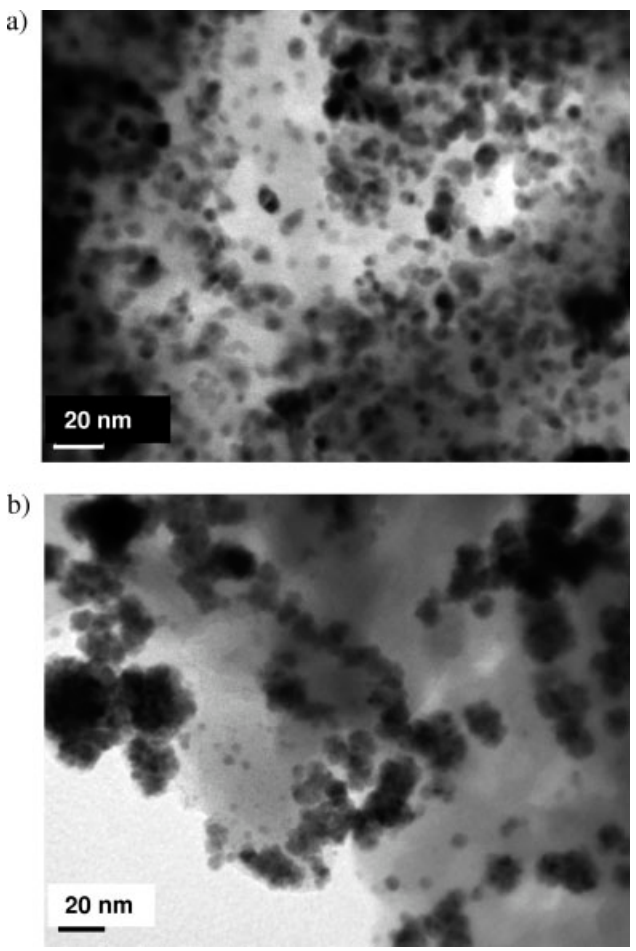

Figure 5 TEM images of PANI–Rh composites containing 0.05 mol Rh per 1 mol of PANI mer prepared in the solutions of the initial $RhCl_3$ concentration equal to (a) 0.67×10^{-3} mol/dm^3, (b) 3.8×10^{-3} mol/dm^3.

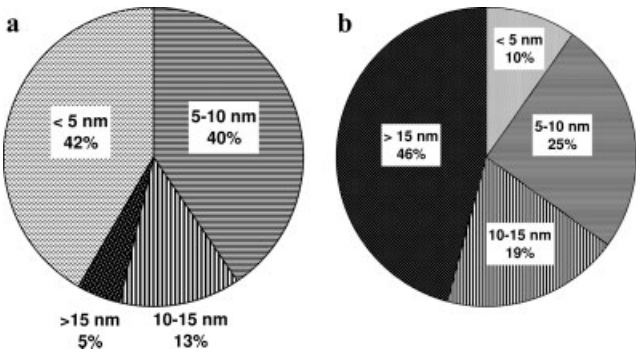

Figure 6 Rh particle size distribution analysis based on TEM images of PANI–Rh composites prepared in the solutions of the initial $RhCl_3$ concentration equal to (a) 0.67×10^{-3} mol/dm^3, (b) 3.8×10^{-3} mol/dm^3.

of various initial concentrations (0.67×10^{-3} mol/dm^3 and 3.8×10^{-3} mol/dm^3). Two features of the samples are most prominent. First, rhodium particles visible in the images as black spots are smaller in the sample obtained at lower $RhCl_3$ concentration in the starting solution. The number of aggregated particles is also smaller in this case. Second, rhodium particles are more uniformly distributed in PANI matrix in the sample prepared at lower $RhCl_3$ concentration in the starting solution. Hence, it can be concluded that for the synthesis of fine Rh particles uniformly distributed in PANI, $RhCl_3$ solutions of low concentrations should be used. Analysis of TEM images has shown that the size of the smallest rhodium particles in the sample prepared in the solution of higher $RhCl_3$ concentration is equal to 2.5 nm, whereas that of the largest ones −50 nm. In the case of the sample obtained in the solution of lower $RhCl_3$ concentration, these values are 1 and 18 nm, respectively.

Additionally, size distribution analysis has been performed by taking into account 250 Rh particles visible in the TEM images of the sample prepared in the solution of higher initial $RhCl_3$ concentration and 400 particles visible in the TEM images of the sample prepared in the solution of lower initial $RhCl_3$ concentration. Results are presented in Figure 6. They show that the former sample contains mainly Rh nanoparticles, whose size does not exceed 10 nm. They constitute 82% of the analyzed particles. The remaining 18% ones are larger than 10 nm. The proportions are opposite in the case of the sample prepared at higher starting $RhCl_3$ concentration in the reducing medium: 75% of the particles larger than 10 nm and 25% smaller than 10 nm.

Thus, based on the studies carried out in the present work it can be concluded that the size and the degree of agglomeration of metallic rhodium particles formed upon reduction of Rh^{3+} ions with $NaBH_4$ in the presence of PANI are controlled by two factors. The first one is Rh content in the sample; the second one is concentration of Rh^{3+} ions in the solution used in the reduction process. The smallest and the least agglomerated particles can be obtained at low amounts of Rh dispersed within the polymer matrix using low concentration of Rh^{3+} ions in the solution (in the present study: 0.05 mol Rh per 1 mol of PANI mer and 0.67×10^{-3} mol/dm^3, respectively).

To find out the changes of PANI chain occurring upon reduction of Rh^{3+} ions in the presence of the polymer, we have investigated PANI–Rh composites using FTIR and N1s spectroscopies. FTIR spectra are collected in Figure 7 in which—for comparison—the spectrum of the starting polymer is included. Analysis of the spectra shows that upon the reduction process some IR bands characteristic for PANI change their positions. This concerns mainly the following bands:

- the band at 1585 cm^{-1} due to quinoid ring C—C and C=N stretching vibrations[34] which shifts to 1575–1572 cm^{-1} in the spectra of PANI–Rh composites;
- the band at 1495 cm^{-1} originating from benzenoid ring C—C stretching vibrations[34] occurring at 1487–1484 cm^{-1} in the spectra of PANI–Rh composites;

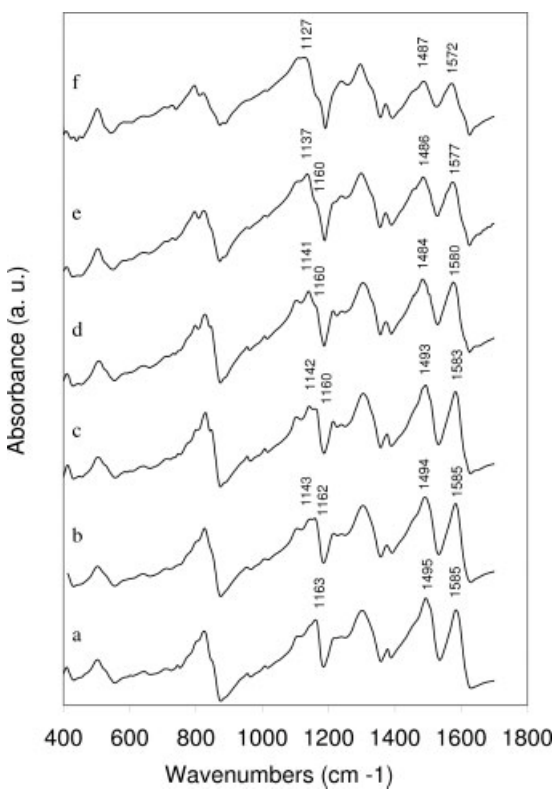

Figure 7 FTIR spectra of (a) PANI and PANI–Rh composites containing different amounts of Rh, (b) 0.05, (c) 0.1, (d) 0.2, (e) 0.5, (f) 1.0 mol per 1 mol of PANI mer.

- the band at 1163 cm^{-1} assigned to CH in-plane deformations[34] which lowers in intensity upon incorporation of Rh into the polymer. Simultaneously, a new band located at 1140–1127 cm^{-1} in the spectra of PANI–Rh composites can be observed.

Such changes in the IR spectra of PANI prove doping (protonation) of the polymer.[34] Most probably, this protonation is due to the reaction between PANI and HCl formed in the course of consecutive reactions taking place in the reducing medium. They are as follows:

$$NaBH_4 + 2H_2O \rightarrow NaBO_4 + H_2$$
$$2[RhCl_3(H_2O)_3] + 3H_2 \rightarrow 2Rh + 6HCI + 6H_2O$$

It should be noted that the signs of PANI protonation in the IR spectra grow as the amount of Rh in the samples increases. Thus, the band originating from quinoid ring C—C and C=N stretching vibrations gradually shifts to lower wavenumbers (1585 cm^{-1}, 1583 cm^{-1}, 1580 cm^{-1}, 1577 cm^{-1}, 1572 cm^{-1} in the spectra of the composites containing 0.05, 0.1, 0.2, 0.5, and 1.0 mol Rh per1 mol of PANI mer, respectively). The growth in intensity of the band at 1140–1127 cm^{-1} due to the protonated segments of PANI with respect to that at 1163 cm^{-1} ascribed to unprotonated ones can be also observed. Since with the increase of the amount of the reduced Rh^{3+} ions, the amount of HCl evolved grows, stronger protonation of the polymer in the composites of higher Rh contents revealed by IR spectroscopy seems to confirm the conclusion that HCl is the protonating agent.

It is worth noting that protonation of PANI has been also established by N1s XPS: spectra of all PANI–Rh composites prepared have contained the components at B.E. values above 400 eV which are due to protonated nitrogen atoms.[35]

Catalytic properties of PANI–Rh composites

Isopropyl alcohol conversion is a useful test to determine activity of various catalysts.[36,37] In the course of this process two parallel reactions take place:

1. dehydration of the alcohol resulting in the formation of propene given by the equation:

$$(CH_3)_2CHOH \rightarrow CH_3CH{=}CH_2 + H_2O$$

2. dehydrogenation of the alcohol leading to acetone in accordance with the following equation:

$$(CH_3)_2CHOH \rightarrow CH_3C(O)CH_3 + H_2$$

Propene is formed on the acidic centres of the catalyst, whereas acetone—on the redox ones. Hence, determination of selectivity of isopropyl alcohol conversion to propene and acetone makes it possible to conclude on acid-base and redox properties of the catalyst surface.

Results of isopropyl alcohol conversion conducted in the presence of PANI–Rh composites containing 0.05 mol Rh per 1 mol of PANI mer prepared in the

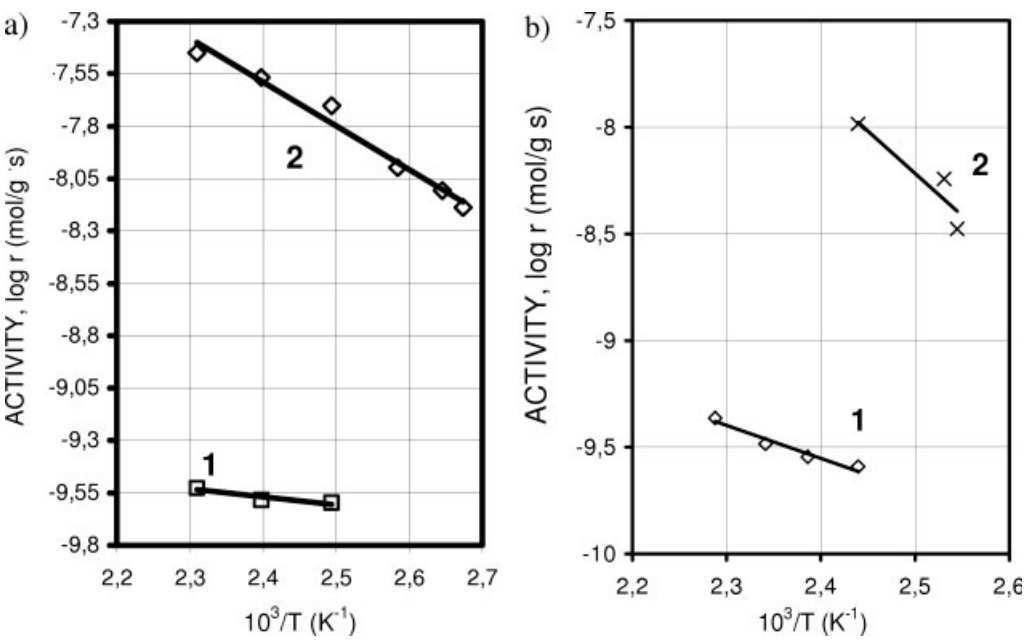

Figure 8 Arrhenius plots of isopropyl alcohol conversion carried out in the presence of PANI–Rh composites containing 0.05 mol Rh per 1 mol of PANI mer in the solutions of the initial $RhCl_3$ concentration equal to (a) 0.67×10^{-3} mol/dm^3, (b) 3.8×10^{-3} mol/dm^3. 1-conversion to propene, 2-conversion to acetone

TABLE I
Selectivity and Activation Energy of Catalytic Isopropyl Alcohol Conversion Performed in the Presence of PANI-Rh Composites Containing 0.05 mol Rh per 1 mol of PANI mer

	Selectivity (%)						Activation energy[a] (kJ/mol)	
	T = 380 K		T = 400 K		T = 420 K			
Sample	Propene	Acetone	Propene	Acetone	Propene	Acetone	E_{a1}	E_{a2}
A	2.0	98.0	1.5	98.5	1.2	98.8	7.4	40.0
B	0.0	100.0	0.0	100.0	2.3	97.7	29.1	75.5

Sample A: prepared in the solution of the initial $RhCl_3$ concentration equal to 0.67×10^{-3} mol/dm^3, Sample B: 3.8×10^{-3} mol/dm^3.

[a] E_{a1} denotes activation energy of dehydration reaction resulting in propene; E_{a2} denotes activation energy of dehydration reaction resulting in acetone.

solutions of various initial $RhCl_3$ concentrations are presented in Figure 8 and Table I. It is seen that both catalysts show mainly redox activity giving predominantly acetone as the product of the catalytic process. Selectivity towards dehydrogenation reaction exceeds 97% in the whole temperature range studied (Table I).

However, significant difference in the redox activity of the catalysts can be observed. The sample prepared in the solution of lower initial $RhCl_3$ concentration is about three times more active than that obtained in the solution of higher initial $RhCl_3$ concentration. Moreover, catalytic dehydration process carried out in the presence of the former sample proceeds in the kinetic region in the whole temperature range studied. In contrast, it transforms into the diffusion region very quickly when the latter sample is applied as the catalyst. This is proved by almost horizontal course of curve 2 in Figure 8(b).

It should be also noted that the activation energy value of the dehydration process proceeding in the presence of more active catalyst (40 kJ/mol, Table I) is characteristic for very active redox catalysts.

There are numerous factors that can affect activity of a supported heterogeneous metal catalyst. Among them, high dispersion of the catalytic centers on the support and their good accessibility for the reacting molecules are very important to obtain an efficient catalyst. Both these factors are influenced by physical properties of a support, that is, its surface area and porosity. Sufficiently high surface area of a support prevents metal particles from aggregation, that is, makes it possible to obtain their high dispersion. On the other hand, the presence of open pores within which catalytic sites are located, and their appropriate sizes for the reacting molecules, provide good accessibility. This is particularly important in the case of branched molecules, such as isopropyl alcohol whose catalytic conversion has been studied in the present work.

Results of the catalytic tests performed indicate that PANI as a support for Rh catalysts shows good physical properties. Under appropriate preparation conditions, samples containing highly dispersed metal nanoparticles exhibiting high catalytic activity in isopropyl alcohol conversion have been obtained. Therefore, the observed differences in the activity of both catalysts studied should be related to the properties of the catalytic centers and not to those of PANI support. They can be explained by differences in the Rh particle size distributions on the support. As has been already stated, the sample prepared in the solution of lower initial $RhCl_3$ concentration has contained predominantly uniformly distributed Rh nanoparticles whose size has been below 10 nm (Figs. 5 and 6). In the other sample, larger, agglomerated particles have been present. Better dispersion of metallic particles resulting in their higher surface area on which the catalytic process can proceed, causes their higher catalytic activity.

CONCLUSIONS

It has been shown that polyaniline (PANI)–rhodium composites can be prepared by simple reduction of Rh^{3+} ions carried out in the presence of the polymer. The size distribution of metallic particles incorporated into PANI matrix depends on the initial concentration of Rh^{3+} in the reducing medium as well as on the Rh content in the sample. The composites containing mainly Rh crystallites whose size has not exceeded 10 nm have been obtained at low concentration of Rh^{3+} ions in the reduced solution (0.67×10^{-3} mol/dm^3) and low Rh content (0.05 mol Rh per 1 mol of PANI mer). They exhibit significantly higher activity in the catalytic isopropyl alcohol conversion process than the composites containing larger Rh particles.

References

1. Gallei, E.; Schwab, E. Catal Today 1999, 51, 535.
2. Zheng, Z.; Feldman, D. Prog Polym Sci 1995, 20, 185.
3. Moszner, N.; Salz, U. Prog Polym Sci 2001, 26, 535.
4. Mucha, M. Prog Polym Sci 2003, 28, 837.

5. MacDiarmid, A. G.; Epstein A. J. Faraday Discuss Chem Soc 1989, 88, 317.
6. Zagorska, M.; Kulszewicz-Bajer, I.; Blet, O.; Zawirska, P.; Dufour, B.; Rannou, P.; Pron, A. Synth Met 2003, 138, 543.
7. Olinga, T. E.; Fraysse, J.; Travers, J. P.; Dufresne, A.; Pron, A. Macromolecules 2000, 33, 2107.
8. Al-Attar, H. A.; Telfach, A. D. Opt Commun 2004, 229, 263.
9. Pron, A.; Nicolau, Y.; Genoud, F.; Nechtschein, M. J Appl Polym Sci 1997, 63, 971.
10. Amarnath, C. A.; Palaniappan, S.; Rannou, P.; Pron, A. J Appl Polym Sci 2007, 103, 1113.
11. Yang, X.; Zhao, T.; Yu, Y.; Wei, Y. Synth Met 2004, 142, 57.
12. Khanna, P. K.; Singh, N.; Charan, S.; Viswanath, A. K. Mater Chem Phys 2005, 92, 214.
13. Kang, Y.-O.; Choi, S.-H.; Gopalan, A.; Lee, K.-P.; Kang, H.-D.; Song, Y. S. J Non-Cryst Solids 2006, 352, 463.
14. Sharma, S.; Nirkhe, C.; Pethkar, S.; Athawale, A. A. Sens Actuators B 2002, 86, 131.
15. Kinyanjui, J. M.; Hanks, J.; Hatchett, D. W.; Smith, A.; Josowicz, M. J Electrochem Soc 2004, 151, D113.
16. Ma, Y.; Li, N.; Yang, C.; Yang, X. Colloids Surf A Physicochem Eng Aspects 2005, 269, 1.
17. Bird, A. J. Gmelin Handbook of Inorganic Chemistry, 8th ed.; Springer-Verlag: Berlin, 1986; Pt Suppl, Vol. A1, p 92.
18. Laborde, H.; Léger, J.-M.; Lamy, C. J Appl Electrochem 1994, 24, 219.
19. Mikhaylova, A. A.; Molodkina, E. B.; Khazowa, O. A.; Bagotzky, V. S. J Electroanal Chem 2001, 509, 119.
20. Kinyanjui, J. M.; Harris-Burr, R.; Wagner, J. G.; Wijeratne, N. R.; Hatchett, D. W. Macromolecules 2004, 37, 8745.
21. Kinyanjui, J. M.; Wijeratne, N. R.; Hanks, J.; Hatchett, D. W. Electrochim Acta 2006, 51, 2825.
22. Tang, Z.; Geng, D.; Lu, G. Thin Solid Films 2006, 497, 309.
23. O'Mullane, A. P.; Dale, S. E.; Day, T. M.; Wilson, N. W.; Macpherson, J. V.; Unwin, P. R. J Solid State Electrochem 2006, 10, 792.
24. Maksimov, Y. M.; Kolyadko, E. A.; Shishlova, A. V.; Podlovchenko, B. I. Russ J Electrochem 2001, 37, 777.
25. Li, H.-S.; Josowicz, M.; Baer, D. R.; Engelhard, M. H.; Janata, J. J. Electrochem Soc 1995, 142, 798.
26. Park, J.-E.; Gil, S.-G.; Koukitu, A.; Hatozaki, O.; Oyama, N. Synth Met 2004, 141, 265.
27. Mourato, A.; Wong, S. M.; Siegenthaler, H.; Abrantes, L. M. J Solid State Electrochem 2006, 10, 140.
28. Zum Mallen, M. P.; Schmidt, L. D. J Catal 1996, 161, 230.
29. Ferreira-Aparicio, P.; Bachiller-Baeza, B.; Rodriguez-Ramos, I.; Guerrero-Ruiz, A.; Fernández-Garcia, M. Catal Lett 1997, 49, 163.
30. Cao, Y.; Andreatta, A.; Heeger, A. J.; Smith, P. Polymer 1989, 30, 230.
31. Wolsey, W. C.; Reynolds, C. A.; Kleinberg, J. Inorg Chem 1963, 2, 463.
32. JCPDS—International Centre for Diffraction Data, database 2002 (www.icdd.com), file 05-0685.
33. NIST Standard Reference Database 20, Version 3.4 (Web Version), released August 2003 (www.nist.gov).
34. Tang, J.; Jing, X.; Wang, B.; Wang, F. Synth Met 1988, 24, 211.
35. Kang, E. T.; Neoh, K. G.; Khor, S. H.; Tan, K. L.; Tan, B. T. G. J Chem Soc Chem Commun 1989, 695.
36. Stochmal-Pomarzańska, E.; Hasik, M.; Turek, W.; Proń, A. J Mol Catal 1996, 114, 267.
37. Mrowiec-Białoń, J.; Turek, W.; Jarzębski, A.B. React Kinet Catal Lett 2002, 76, 213.